International Journal of Mechanical, Industrial and Aerospace Sciences
ISSN: 2517-9950
Vol:7, No:12, 2013

Performance Evaluation of Extruded-Type Heat Sinks Used in Inverter for Solar Power Generation

Jeong Hyun Kim, Gyo Woo Lee

***Abstract*—**In this study, heat release performances of the three extruded-type heat sinks can be used in inverter for solar power generation were evaluated. Numbers of fins in the heat sinks (namely E-38, E-47 and E-76) were 38, 47 and 76, respectively. Heat transfer areas of them were 1.8, 1.9 and 2.8m^2. The heat release performances of E-38, E-47 and E-76 heat sinks were measured as 79.6, 81.6 and 83.2%, respectively. The results of heat release performance show that the larger amount of heat transfer area the higher heat release rate. While on the other, in this experiment, variations of mass flow rates caused by different cross sectional areas of the three heat sinks may not be the major parameter of the heat release. Despite the 47.4% increment of heat transfer area of E-76 heat sink than that of E-47 one, its heat release rate was higher by only 2.0%; this suggests that its heat transfer area need to be optimized.

***Keywords*—**Solar Inverter, Heat Sink, Forced Convection, Heat Transfer, Performance Evaluation.

I. Introduction

THE power generation system is needed to transform several energies into electric energy. Particularly, there is an inverter in the solar power generation system which plays an important role in converting the direct current (DC) generated from photovoltaic solar cell into the utility frequency alternating current (AC) that can be fed into a commercial electrical grid or used by a local, off-grid electrical network. It is a critical component in a photovoltaic system, allowing the use of ordinary commercial appliances. The inverter has high converting speed power semiconductors, namely insulated gate bipolar transistors (IGBTs), which are essential element in the inverter. The power loss from the IGBT turns into heat and increases the junction temperature inside the chip. This degrades the characteristics of the device and shortens its life. It is important to release the heat produced from the chip junction to lower the junction temperature [1]. That is why the IGBT packed with heat sink system. The selection of proper heat sink depends on the temperature range of the heat source, an amount of heat to be released, ambient conditions, and so on.

There are lots of works related with various heat sinks. In 2004, Lee [2] showed the design of a heat dissipation system is consist of a heat source, a heat sink and a fan for the forced air cooling for the 400 kW IGBT inverter. He did both experimental and simulation studies, and showed that the differences between them were less than 10%. Similarly, Jeon et al. [3] examined the effects of temperature increment of the serially aligned heat sources on the heat release performance of the tunnel-type air-cooled heat sink. Also, they presented the example design of heat release system by using the empirical relation came from the experiment. While, Kim et al. [4] developed the heat release system for the deep-focused solar cell modules having heat spreaders and heat sinks. They also reported the empirical relation can be used for the estimation of heat release performance of the natural convection heat sink. In 1996, Shaukatullah et al. [5] reported an optimized design of pin-fin heat sink for use in low velocity applications where there is plenty of open space around for the air to bypass the heat sink. While, in 2002, Kim et al. [6] investigated the thermal performance of several heat sinks such as extruded, aluminum foam, and layered one. Lee [7] reported the optimization of heat sink with pressure drop and heat transfer area. The pressure drops and heat transfer areas were varied by changing the number of fins. Riu et al. [8] evaluated the performance of a heat sink with strip-shaped fin, and tried to determine the optimal geometry.

In this experiment, we investigated the performances of the three extruded-type heat sinks developed for use in the inverter of solar power generation. The three extruded-type heat sinks have 38, 47 and 76 fins having the same external dimension.

II. Experimental

A. Experimental Setup

Fig. 1 shows the experimental setup used in this study. The figure has top and side views showing locations of thermocouples, heat sources, and fans. The lower part of the figure shows the sectional views of this experimental setup. The Experimental setup is consist of a heat sink, three heat sources, two induction fans, inlet (Φ 0.25m) and exit (Φ 0.20m) flow ducts, data acquisition system, several thermocouples and others.

Three aluminum blocks having six cartridge heaters on the upper plate of the heat sink used as substitutes for IGBTs in the commercial inverter. They have a total power consumption of 1905 Watt, and have a dimension of 60mm (W) x 140mm (L) x 20mm (H) in each. Thermal grease (G-747, Shinetsu Co.) was used on the surface of cartridge heaters and spaces between aluminum blocks and upper plate of heat sink to enhance the heat transfer among them. Those heating blocks are positioned and shown in Fig. 1.

J. H. Kim is Graduate School Student with the Division of Mechanical Design Engineering, Chonbuk National University, Jeonju, Jeonbuk 561-756, South Korea (e-mail: chemist@jbnu.ac.kr).

G. W. Lee is Associate Professor with the Division of Mechanical Design Engineering, Chonbuk National University, Jeonju, Jeonbuk 561-756, South Korea (Corresponding Author e-mail: gwlee@jbnu.ac.kr).

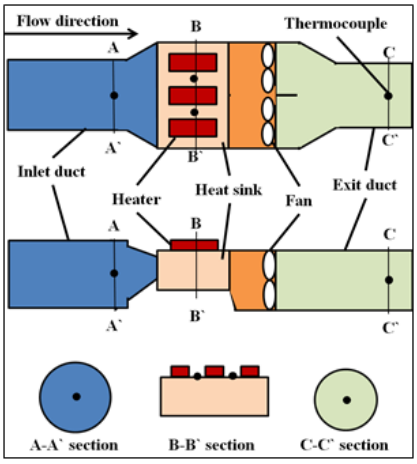

Fig. 1 A schematic of the experimental setup

The cooling air is flowed into the heat sink from the ambient, heated by the upper plate and fins, and then exhausted to the outside thru the duct. Several dot marks near the heat sink in Fig. 1 are locations of thermocouples for measuring the heat transfer thru the heat sink. The T-type thermocouples (TG-T-36-500, Omega Co.) are made and used after the calibration. The temperatures from the thermocouples were converted to digital data thru the A/D converting device (34970A with 34902A module, Agilent Technologies) and saved in the computer.

Two fans that are used in this experiment have a maximum flow rate (that is, zero pressure drop) of 710 m^3/hr in each. Fans are installed parallel as shown in Fig. 1. Since the cross sectional areas of the three heat sinks were varied, the pressure drops and mass flow rates of the air flow thru the heat sinks were changed.

To calculate the mass flow rate, the air velocity induced thru the inlet duct was measured at the center of the location of 800 mm behind the entrance of inlet duct by the velocity meter. With an assumption of fully-developed flow, the mass flow rate might be calculated from density of air, cross sectional area and averaged velocity of air. The averaged air velocity can be calculated from the measured maximum air velocity and the corresponding conversion ratio [9] varied with Reynolds number. In this experiment, the conversion ratio ranged from 0.827 to 0.829. Generally, to use the fully-developed flow assumption the ratio of length to diameter (L/D) of duct should exceed 20. In this experiment, due to the restriction of indoor space and the big pressure drop might be caused by the long inlet duct, the ratio is maintained less than 6. So, the actual mass flow of the air thru the heat sink can be slightly larger than that of measured in this experiment.

Partial photos of the three extruded-type heat sinks used in this experiment are shown in Fig. 2. All of them are made of aluminum (AL6061). Because they are manufactured by extrusion, fins and upper plate are a single body. An acrylonitrile lower plate is fabricated separately and assembled together. Detailed specifications of the three heat sinks are written in Table I. All the heat sinks have same exterior dimension. But they have different number of fins, heat transfer area, flow cross sectional area, thickness of fin, fin spacing, height of fin and fin spacing. In the name of the heat sink, E and the following number stand for the extrusion and number of fins, respectively.

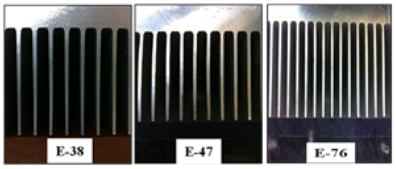

Fig. 2 Photos of the extruded-type heat sinks

B. Experimental Method

In this experiment, the heat sink was cooled down by the forced convection using two fans. The heat release performance of the heat sink was measured by using a heat input of the three heaters on the heat sink and an amount of heat transfer thru the heat sink. The measured heat input, that is, the electricity consumption of the three heaters on the heat sink, was 1904.8 Watt. The temperature difference between inlet and exit temperatures of cooling air gave the information about the amount of heat release thru the heat sink.

Temperature measurement was done every 5 seconds. After 90 minutes from the fan operation, the system was fully reached the first steady state. Since the steady state, averaged inlet and exit air temperatures and the differences were measured and calculated during another 90 minutes as shown in Fig. 3. The second steady state might be measured less 20 minutes from the heater operation in Fig. 3. In this experiment, when the standard deviation of 10-minute averaged temperature was less than 0.5°C we considered it as the steady state.

TABLE I
SPECIFICATIONS OF EXTRUDED-TYPE HEAT SINKS

Name of heat sink		E-38	E-47	E-76
Number of fin		38	47	76
Heat sink	Length [㎜]	325	325	325
	Width [㎜]	400	400	400
	Height [㎜]	100	100	100
Thickness of upper plate [㎜]		18	18	12
Fin spacing [㎜]		11	8.5	5.5
Thickness of fin [㎜]		2.5	2.2	1.5
Height of fin [㎜]		65	55	55
Heat transfer area [㎡]		1.8	1.9	2.8
Flow cross-sectional area [㎡]		0.020	0.016	0.016

Using an equation as below [10], the amount of heat transfer thru the heat sink was calculated. Here, $\dot{Q}$, $\dot{m}_{air}$, C_p, and ΔT denote heat transfer rate (W), mass flow rate of air (kg/s), specific heat at constant pressure (J/kg · K), and temperature

difference between inlet and exit air of a heat sink (K), respectively.

$$\dot{Q} = \dot{m}_{air} \cdot C_p \cdot \Delta T$$

III. Results and Discussion

A. Data Processing

Fig. 3 shows one of the raw data of inlet and exit temperatures of a heat sink throughout the entire operation. Based on these raw data, we got average temperatures and temperature differences. The temperature distribution of the first 90 minutes in Fig. 3 (dotted line marked) shows the initial temperature change caused by the increment of internal energy of air which is transferred from the fan operation to cooling air. After this first steady state the three heaters are turned on.

Details of the initial steady state are shown in Fig. 4. In the case of Fig. 4, the initial temperature rise due to the fan operation is about 0.7°C. To measure and calculate the accurate amount of heat transfer by the heat source only, this temperature increment by fans need to be eliminated from the measured temperature difference between inlet and exit air at the second steady state.

B. Results and Discussion

In Fig. 5, upper plate temperatures, inlet ambient air temperatures and temperature differences between inlet and exit of the three heat sinks are shown. The averaged inlet temperature and standard deviation were 20.51°C and 0.09°C, respectively. The largest temperature difference and its deviation were measured in E-76 heat sink as 8.95°C and 0.14°C, respectively. In case of E-38 heat sink, the smallest temperature difference and its deviation were measured as 7.10°C and 0.09°C, respectively. It is easily seen that as the number of fins in a heat sink is increased its heat transfer area, temperature difference between inlet and exit, and heat release fraction tend to be increased while the temperature of upper plate is decreased. Based on the heat transfer areas in Table I and measured mass flow of air, qualitative analyses are given in Figs. 6 and 7.

Using (1), the amounts of heat release and mass flow rates thru the heat sink were measured and calculated as shown in Fig. 6. The mass flow rates of E-38, E-47, and E-76 heat sink were 0.212, 0.199, and 0.176 kg/s, respectively. At the same time, the amounts of heat release for the three heat sinks were increased as 1516.64, 1544.03, and 1585.48 Watts, respectively. Decrement of the mass flow rates for E-47 and E-76, based on that of E38 heat sink, reached to 6.1% and 17.0%, respectively. But, the amounts of heat transfer of E-38 and E-47 were increased by 2.5% and 4.6% than that of E-38. From this, we believe that, in this condition of experiment, variations of mass flow rates caused by different cross sectional areas of the three heat sinks may not be the major parameter of the heat release performance.

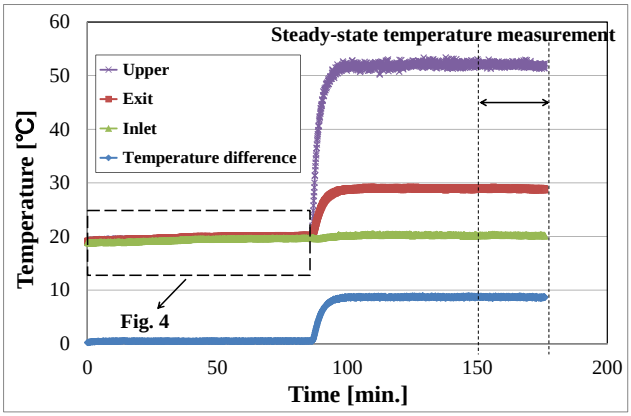

Fig. 3 Distributions of transient temperatures of a heat sink showing the period of steady-state temperature measurement

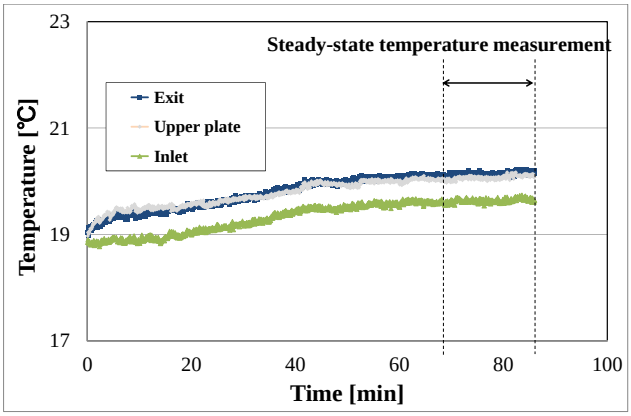

Fig. 4 Distributions of transient temperatures of a heat sink before the heating showing the period of steady-state temperature measurement

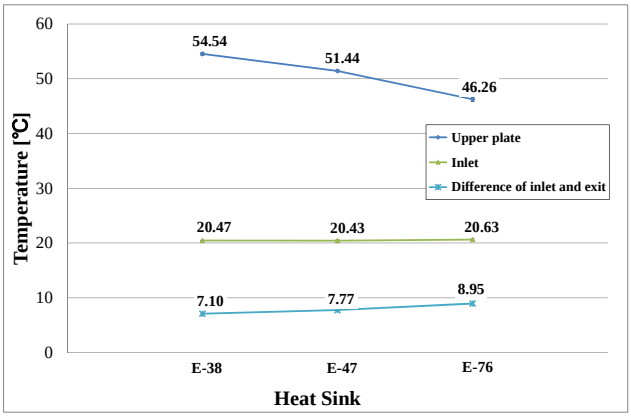

Fig. 5 Temperatures of upper plate and inlet, and the temperature differences of the four heat sinks

Another important parameter for the heat release performance might be the heat transfer area. In Fig. 7 we can see the heat release fraction and the heat transfer areas for the three heat sinks. Heat release fraction has the same meaning as the amount of heat transfer in Fig. 6. Heat transfer areas of the three heat sinks, E-38, E-47 and E-76, were 1.8, 1.9 and 2.8 m^2,

respectively. As the heat transfer areas of E-47 and E-76 heat sink are increased by 5.6% and 55.6% based on that of E-38, the amounts of heat release are also increased by 2.5% and 4.6% based on that of E-38. That is, the larger heat transfer area caused by increased fin number makes the more heat released from the heat sink. So, it is believe that the heat transfer area is the major parameter for the heat release performance in this experiment. But, in spite of relatively larger increment in heat transfer area of E-76 heat sink than that of E-47 heat sink, the amount of heat transfer was increased not much. Therefore, it seems that the optimization of the heat transfer area is needed.

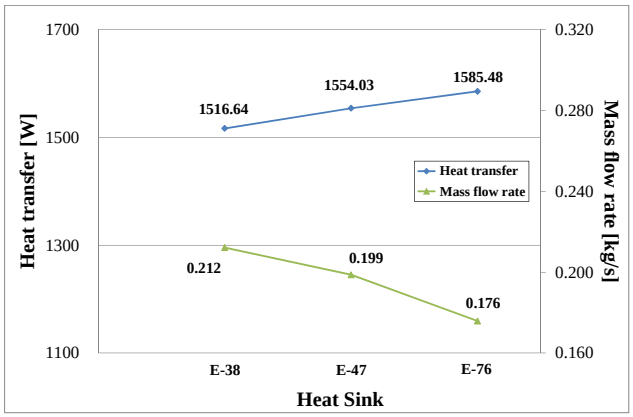

Fig. 6 Heat transfers thru the heat sinks and the mass flow rates of the four heat sink

IV. Conclusion and Plans

In this experiment, we investigated the heat release performance of the three extruded-type heat sinks can be used in the inverter of solar power generator. The heat sinks have 38, 47 and 76 fins. The heat release performances of E-38, E-47 and E-76 heat sinks were measured as 79.6, 81.6 and 83.2%, respectively. The results of heat release performance show that the larger amount of heat transfer area the higher heat release rate. While on the other, in this experiment, variations of mass flow rates caused by different cross sectional areas of the three heat sinks may not be the major parameter of the heat release. Furthermore, in spite of relatively larger increment in heat transfer area of E-76 heat sink than the other, the amount of heat transfer was increased not much. Therefore, it seems that the optimization of the heat transfer area is needed.

In the future, we may assess the additional parameters for the optimized heat sink having better heat release property.

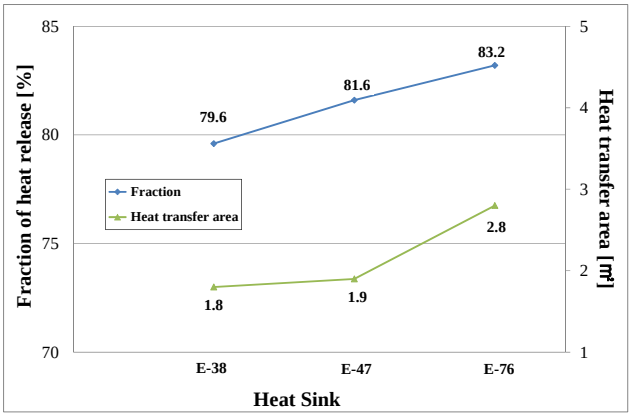

Fig. 7 Heat release fractions thru the heat sinks, and heat transfer areas of the four heat sinks

Acknowledgment

This Following are results of a study on the "Leaders Industry-university Cooperation" Project, supported by the Ministry of Education, Science & Technology (MEST).

References

[1] E. Santi, A. Caiafa, X. Kang, J. L. Hudgins, and P. R. Palmer, D. Goodwine, and A. Monti, "Temperature Effects on Trench-Gate Punch-Through IGBTs," *IEEE Trans. on Industry Applications*, Vol. 40, No. 2, pp. 472~482, 2004.
[2] J. W. Lee, "Design of a Heat Dissipation System for the 400kW IGBT Inverter," *The Trans. of the KIPE*, Vol. 9, No. 4, pp. 350~355, 2004.
[3] C. S. Jeon, Y. K. Kim, J. Y. Lee, and S. H. Song, "Cooling of an In-line Array of Heat Sources with Air-Cooled Heat Sinks," *Trans. Korean Soc. Mech. Eng. B*, Vol. 22, No. 2, pp. 229~234, 1998.
[4] T. H. Kim, K. H. Do, B. I. Choi, Y. S. Han, and M. B Kim, "Development of a Cooling System for a Concentrating Photovoltaic Module," *Trans. Korean Soc. Mech. Eng. B*, Vol. 35, No. 6, pp. 551~560, 2011.
[5] H. Shaukatullah, W. R. Storr, B. J. Hansen, and M. A. Gaynes, "Design and Optimization of Pin Fin Heat Sinks for Low Velocity Applications," *IEEE Trans. on Components, Packaging and Manufacturing Technology-Part A*, Vol. 19, No. 4, pp. 486~494, 1996.
[6] J. H. Kim, J. H. Yun, and C. S. Lee, "An Experimental Study on the Thermal Resistance Characteristics for Various Types of Heat Sinks," *SAREK*, Vol. 14, No. 8, pp. 676~682, 2002.
[7] S. Lee, "Optimum Design and Selection of Heat Sinks," *IEEE Trans. Components, Packaging and Manufacturing Technology-Part A*, Vol. 18, No. 4, pp. 812~817, 1995.
[8] K. J. Riu, C. W. Park, H. W. Kim, and C. S. Jang, "Cooling Characteristics of a Strip Fin Heat Sink," *Trans. Korean Soc. Mech. Eng. B*, Vol. 29, No. 1, pp. 16~26, 2005.
[9] F. M. White, "Fluid Mechanics," 5th ed., McGraw-Hill, 2011.
[10] F. P. Incropera, D. P. DeWitt, T. L. Bergman, and A. S. Lavine, "Introduction to Heat Transfer," 5th ed., John Wiley and Sons, 2006.